CHAPTER VI

NUMERICAL METHOD AND ANALYSES

The development of numerical or FEM analysis for geotechnical engineering works has encouraged the underground constructions in complicated and difficult subsoil condition areas, i.e. metropolis zones. The principle advantages of the FEM analysis are that the interaction between soil and structure can be modeled and that both design loads and expected moments can be studied. Nowadays, there are many finite element and finite difference codes that can be used in analysis of tunnel construction in various subsoil conditions.

The finite element program called PLAXIS version 8 (Brinkgreve, 2002), licensed to Chulalongkorn University, is proposed to be used in this research. It is a finite element package specifically intended for the 2D analysis of deformation and stability for various types of geotechnical works. The word PLAXIS is an abbreviation of "pla" from the word plane strain and "axis" from axisymmetric analysis, which are generally used in geotechnical field. The plane strain model is considered when the analysis problems, i.e. tunnel or embankment, have a constant cross section for a distance in which the movements perpendicular to the section are assumed to be zero. However, the axisymmetric option is selected when the analysis problem is symmetric around the central axis and the stress state and movement can be considered identically at any distance from that axis.

This chapter provides an overview of the PLAXIS program and the specific options of the implementation of PLAXIS program for the analysis in this research. It also gives some examples of recent research studies using PLAXIS program as well as the Mohr Coulomb soil model, which is also selected for the present study. The final section provides the analysis method this study used.

6.1 Sign Conventions and Units

6.1.1 Sign Conventions

The geometry model is necessary for the subsequent input and calculation. This geometry is created in the *x-y* plane of the global coordinate system (Figure 6.1), where the *z*-direction is the out-of-plane direction with the positive direction is pointing towards users. Although PLAXIS version 8 is a 2D program, stresses are based on the 3D Cartesian coordinate system as shown in Figure 6.1. In a plane strain analysis σ_{zz} is the out-of-plane stress. In an axisymmetric analysis, x represents the radial coordinate, y the axial coordinate and z the tangential direction. In this case, σ_{xx} represents the radial stress and σ_{zz} the hoop stress.

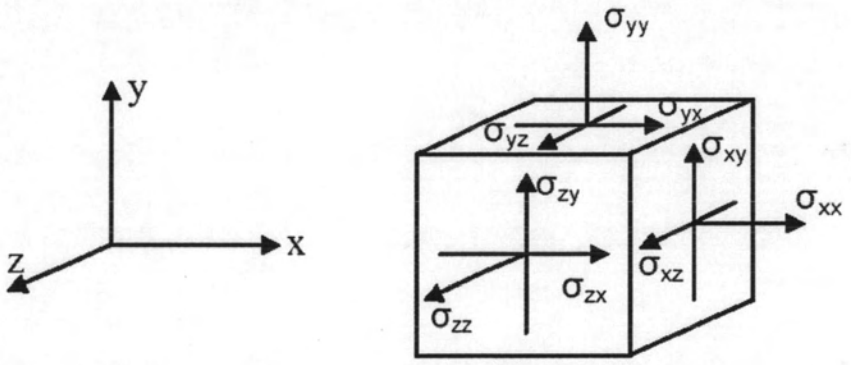

Figure 6.1 Coordinate system and sign conventions for stress components (Brinkgreve, 2002)

Figure 6.1 shows the positive stress directions in the global coordinate system. Therefore, the compressive stresses and forces as well as pore pressures resulting from a calculation are mentioned with the negative signs while the tensile stresses and forces are mentioned with the positive one.

6.1.2 Units

In PLAXIS program, the basic units can be found in the ***General settings window*** of the Input program. By default, these basic units are set to m, kN and day for length, force and time, respectively. Therefore, it is necessary to select an appropriate set of basic units before starting to analyze a new problem. However, the

basic units can be changed at any time before processing to the calculation. The new units will also be automatically considered for all the input values in the input program.

In a plane strain analysis, the computed forces resulting from prescribed displacements represent forces per unit length in the out of plane direction (z-direction, Figure 6.1).

In an axisymmetric analysis, the computed forces (***Force-X, Force-Y***) are those that act on the boundary of a circle subtending an angle of one radian. In order to obtain the forces corresponding to the complete problem, these forces must be multiplied by a factor of 2π. All other outputs for axisymmetric problems are given per unit width and not per radian.

6.2 Geometric Input

The problem to be analyzed in PLAXIS is represented by a geometry model, which consists of points, lines and clusters. Points and lines are entered by users based on the drawing procedures while the clusters are automatically generated by the program. Moreover, structural components or special conditions can be directly assigned to the geometry model to simulate tunnel linings, walls, plates, soil-structure interaction or loadings.

It is, therefore, recommended that the creation of a geometry model be started from drawing the full geometry contour. In addition, users may specify material layers, structural members, lines used for construction phases, loads and boundary conditions. The geometry model should not only include the initial situation, but also situations that occur in the various calculation phases. When the full geometry model has been defined and the material properties have assigned to all the geometry components, the finite element mesh can be easily generated.

6.3 Mesh Generation

When the geometry model is fully defined and material properties are assigned to all clusters and structural members, the geometry has to be divided into finite elements in order to perform finite element calculations. A composition of finite

elements is called a mesh. The basic type of element in a mesh is the 15-node triangular element or the 6-node triangular element (section 6.4).

PLAXIS allows a fully automatic generation of unstructured meshes of triangular elements. A precious time is saved by this automatic mesh generation. The options for global and local mesh refinement are available during phase. When the global refinement is selected, the mesh is automatically generated one more again and the global coarseness parameter will be increased one level for example from medium to fine. However, the local refinement is usually applied to the areas where large stress concentrations or large deformation gradients are expected. This situation often occurs when the geometry model includes edges or corners or structural members.

6.4 Elements and Accuracy of Calculation

To analyze a problem, users may select either 15-node or 6-node triangular elements (Figure 6.2) as the basic type of element to model soil layers and other volume clusters. A 6-node triangular element consists of 6 nodes and contains 3 stress points while a 15-node triangular element consists of 15 nodes and contains 12 stress points. The type of element for structures and interfaces is automatically taken to be compatible with the basic type of soil element. A mesh composed of 15-node elements usually gives a much finer distribution of nodes and thus much more accurate results than a similar mesh composed of an equal number of 6-node elements. In addition, in axisymmetric models or in the case of a bearing capacity calculation or a safety analysis by means of phi-c reduction, the 6-node elements usually yield an overprediction resulting in the failure loads or safety factors. Nevertheless, the use of 15-node elements is more time consuming than using 6-node ones.

During a finite element calculation, displacements are calculated at the nodes. On the contrary, stresses and strains are calculated at individual stress points (Gaussian integration points) rather than at the nodes.

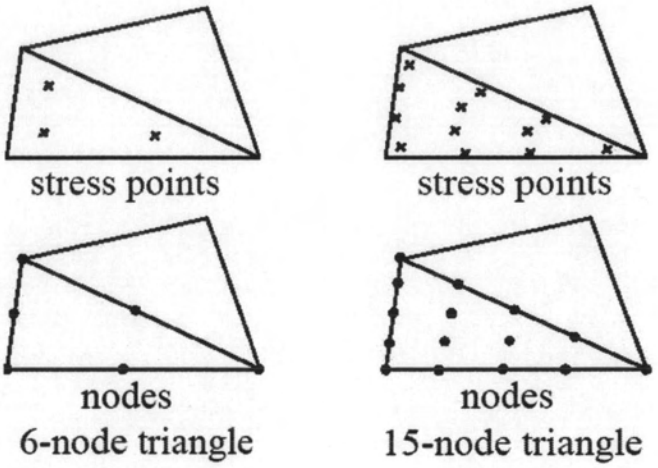

Figure 6.2 Nodes and stress points in soil elements (Brinkgreve, 2002)

6.5 Structural Elements

In PLAXIS, the structural elements could be simulated as line elements (plates or beam elements) with three degrees of freedom per node: Two degrees of freedom related to the displacement (u_x, u_y) and one rotational degree of freedom (rotation in the *x-y* plane: ϕ_z). Whenever the 6-node soil elements are used, the 3-node beam elements are automatically considered and each beam element contains two pairs of Gaussian stress points. On the other hand, when the 15-node soil elements are used, the 5-node beam elements are considered with four pairs of stress points as shown in Figure 6.3.

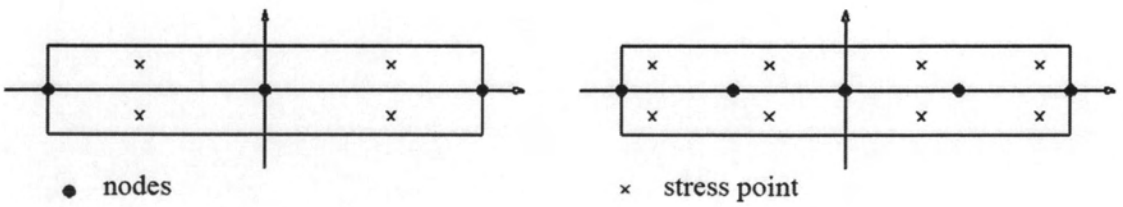

Figure 6.3 Position of nodes and stress points in a 3-node and a 5-node beam element (Brinkgreve, 2002)

The most important parameters of beam elements are the flexural rigidity (bending stiffness) EI and the axial stiffness EA. From these two parameters, an equivalent thickness, d_{eq}, of beam element can be determined based on Equation (6.1).

$$d_{eq} = \sqrt{12\frac{EI}{EA}} \tag{6.1}$$

Attention must be paid when the beam elements are used to represent the embedded structures since they will superimpose on the soil layers. Therefore, the effective beam weight has to be considered in the analysis (Brand, 2000).

Beam elements can be activated or de-activated in calculation phases using Staged construction as loading input.

6.6 Interfaces

The interface elements are needed for calculations involving soil-structure interaction. They may be used to simulate, for example, the thin zone of intensely shearing material at the contact between a tunnel and the surrounding soil. The absence of interface between soil and structure may lead to an unrealistic stress distribution, especially for the structure involving edges or corners.

The interface properties are calculated from the surrounding soil properties in the associated data set and the strength reduction factor (R_{inter}). In the case $R_{inter} < 1$, this means that the properties of interface such as friction, cohesion and stiffness are lower than the surrounding soil properties. In contrast, the same properties for both interface and surrounding soils are executed if $R_{inter} = 1$. In the absence of detailed information, the value of R_{inter} may be assumed in an order of 2/3 for a sand-steel contact and of the order of 1/2 for clay-steel contact, whereas the interaction with rough concrete usually gives a somewhat higher value. A value of R_{inter} which is greater than 1 is not normally used.

6.7 Soil Models

The PLAXIS version 8 provides a wide range of soil models to be used for analysis a specific problem. These soil models could be cited as linear elastic, Mohr-

Coulomb, jointed rock, hardening-soil, soft-soil creep and soft soil. Moreover, this updated version offers a special option named "user-defined soil models" that allows users to implement a wide range of constitutive soil models, which are not available, into the PLAXIS program.

A brief description of the six soil models is given in the following paragraphs; however, a deeper explanation about Mohr Coulomb soil model which is chosen for this study is extended in section 6.11.1.

Linear elastic model: This model involves only two elastic parameters, i.e. Young's modulus E and Poisson's ratio ν. The model created is based on Hooke's law of isotropic linear elasticity, which could not simulate the real behavior of soil. Generally, it is not considered using with soft rock but it is suitable to model the massive structural elements in soil and bedrock layers.

Mohr-Coulomb model: This elastic perfectly-plastic model is very well known and habitually used for a preliminary analysis of the problem to be studied. Basically, the model involves five parameters, in which two parameters, Young's modulus E and Poisson's ratio ν, control the elastic behavior, and other three, cohesion c, friction angle φ and angle of dilatancy ψ, control the plastic behavior. In addition, a proper K_0-value has to be mentioned in order to calculate the initial horizontal stress which plays an important role in soil deformation problems.

Joint rock model: The model is an anisotropic elastic perfectly-plastic model, which is used to simulate the behavior of rock layers involving stratification and particular fault directions. Materials may have different properties in different directions. The intact rock is anticipated to behave fully elastically with constant stiffness properties E and ν. A reduction of elastic properties may be defined for the stratification direction.

Hardening-soil model: In the same way as Mohr-Coulomb model, the limited states of stress of hardening-soil model are also described by cohesion c, friction angle φ and angle of dilatancy ψ. However, soil stiffness is classified into three different kinds of stiffness: the triaxial loading stiffness, E_{50}, the triaxial unloading stiffness, E_{ur}, and the oedometer loading stiffness, E_{oed}. The hardening-soil model can be used to simulate the behavior of soft and stiff soil as well.

Soft-soil creep model: Unlike the above hardening-soil model, the soft-soil creep model also takes in to account the effect of viscosity, i.e. creep and stress

relaxation. In fact, all soils exhibit some creep and primary compression is thus followed by a certain amount of secondary compression. The model may be used to simulate the time-dependent behavior of near-normally consolidated clays, clayey silts and peat.

Soft soil model: It is a Cam-Clay type model since the basic parameters (λ^* and κ^*) of this model are linked to those (λ and κ) of the Cam-Clay via the void ratio parameter. The model can be used to simulate the behavior of primary compression of normally-consolidated clay soils. However, it does not incorporate time effects such as in secondary compression, which is available in the soft-soil creep model described previously.

6.8 Automatic Load Stepping

The PLAXIS program enables this feature to optimize the step size in order to get an efficient and robust calculation process for plastic calculations. The automatic load stepping procedures are controlled by a number of calculation control parameters. There is a convenient default setting for most control parameters, which strikes a balance between robustness, accuracy and efficiency. However, users can influence the automatic solution procedures by manually adjusting the control parameters. In this way it is possible to have a stricter control over step sizes and accuracy.

6.9 Staged Construction

This important feature enables a realistic simulation of construction and excavation processes by activating and deactivating clusters of elements, applying loads, changing water tables, etc. This procedure allows for a realistic assessment of stresses and displacements as caused, for example, by soil excavation during an underground construction project. It is also possible to change the material data set of a plate or cluster in the framework of this staged construction. However, the ratio *EI/EA* which determines the equivalent plate thickness (Equation 6.1) must not be changed, since this will introduce an out-of-balance force.

6.10 Upgraded Lagrangian Analysis

With this option, the finite element mesh is continuously updated during the calculation. For some situations, a conventional small strain analysis may show a significant change of geometry. In these situations it is advisable to perform an updated mesh or updated Lagrangian calculation, which is available for all types of calculations. However, one should notes that an updated mesh analysis takes much more time and is less robust than a normal calculation. Hence, this option should only be used in special cases such as the construction of an embankment on soft soil.

6.11 Mohr Coulomb Model and Analysis Options

6.11.1 Mohr Coulomb Model

The Mohr-Coulomb model is a well-known soil model that can be used as a first order approximation of real soil behavior, which generally behaves a highly non-linear under load. This robust and simple non-linear model is based on soil parameters known in most practical situations, which lead to a quick and simple analysis; moreover, the procedure tends to reduce errors.

The selection of this model for analyses of the current research based on some reasonable arguments:

- As mentioned in the previous paragraph (section 6.7), the model needs only five basic soil parameters, which are very familiar with the geotechnical engineers, and can be obtained based on the simple field or laboratory tests. Unlike other advanced soil models, which need more tests and sometime complicated in terms of test procedure as well as the availability of test equipment.
- Unlike other advanced soil models, which usually take more time for computation, the model is relatively simple so it leads to a reduction of errors and quick analysis.
- The model can provide a better soil behavior than the linear elastic model, which is generally too crude to capture real behavior of soil.
- It is clearly mentioned in the material manual of PLAXIS version 8 that in unloading problems such as excavation works and tunneling, the soft-soil creep model does not provide a better prediction than the Mohr-Coulomb

model. On the other hand, the soft soil model is also certainly not recommended to use in excavation problems.

Accordingly, it is possible that this elastic-plastic model, Mohr Coulomb model, has been extensively used collaboratively with the PLAXIS program in several research studies and in practices related to the underground constructions. For example, based on the PLAXIS program, Mohr Coulomb model has been used for such recent research studies as mentioned in the last section of this chapter, section 6.12.

Figure 6.4 illustrates the real soil behavior resulting from standard drained triaxial tests and the idealized form given by the Mohr Coulomb model. The figure gives an indication of the meaning and influence of the five basic model parameters. The irreversible strain is noticeably happened when the yield point is reached as shown in Figure 6.4b and the dilatancy angle ψ is needed to model the irreversible increase in volume.

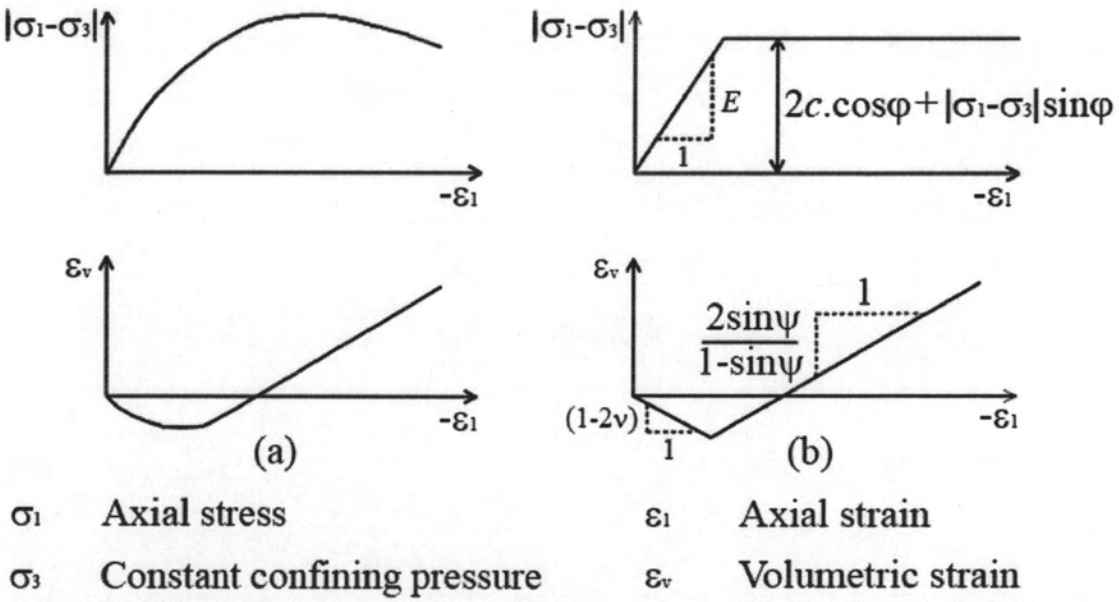

Figure 6.4 Results from standard drained triaxial tests (a) and Mohr Coulomb model (b) (Brinkgreve, 2002)

In the data set of Mohr Coulomb soil model, PLAXIS provides another option that users can enter the value of shear modulus G or the oedometer modulus E_{oed} as

alternatives to substitute the Young's modulus parameter (E). The relationship between these stiffness moduli is given by:

$$G = \frac{E}{2.(1+\nu)} \tag{6.2}$$

$$E_{oed} = \frac{(1-\nu).E}{(1-2.\nu).(1+\nu)} \tag{6.3}$$

When formulated in terms of principal stresses, the Mohr-Coulomb failure criterion consists of six yield functions. In principal stress space these yield functions represent the surface of an irregular hexagonal pyramid as shown in Figure 6.5. This figure describes yield surface for the case of cohesionless soil such as sand. In the case of undrained cohesive soils, the convergent point of the yield surfaces will not start from the origin of the coordinate system but from a point behind that origin. The linear elastic behavior is located in side the yield surface.

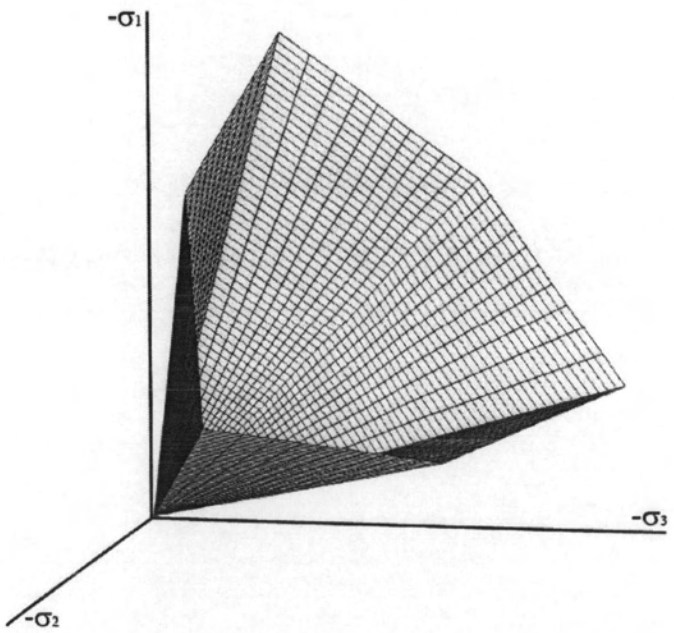

Figure 6.5 Mohr Coulomb yield surface in principal stress space for cohesionless soil (Brinkgreve, 2002)

As the major ground displacement response to bored tunnel occurred in the short-term condition (Teparaksa 2005a and b, and Phenwej et al. 2006), the undrained analyses were appropriate for the cohesive soil layers. There are two options available in PLAXIS for users to perform the undrained analyses, and they are described in section 6.11.2 and 6.11.3.

6.11.2 Undrained Analysis with Effective Parameters

The simulation of undrained behavior by using effective model parameters is the first option provided by PLAXIS. This option is available for all material models and can be carried out by specifying the ***type of material behavior*** as ***undrained***. In this analysis, the grain solid of the soil or soil skeleton and pore water are supposedly two separate elements, which share the same physical space.

The pore pressures between the grain solid of a soil body, usually caused by water, contribute to the total stress level. According to the basic principle of Terzaghi, total stress σ can be divided into effective stress σ' and pore pressures u. However, water is supposed not to sustain any shear stress, so the effective shear stress is equal to the total shear stress. Therefore, the effective shear modulus is equal to the total effective shear modulus accordingly.

Once this special option is selected, the program will convert the input effective parameters such as G and ν' into the undrained parameters E_u and ν_u according to Equation (6.4) to (6.7).

$$E_u = 2.G.(1+\nu_u) \tag{6.4}$$

$$\nu_u = \frac{\nu'+\mu(1+\nu')}{1+2\mu(1-2\nu')} \tag{6.5}$$

in which

$$\mu = \frac{1}{3n}\frac{K_w}{K'} \tag{6.6}$$

where K_w is the bulk modulus of water and the bulk modulus of soil skeleton (K') can be obtained by

$$K' = \frac{E'}{3(1-2\nu')} \tag{6.7}$$

A fully incompressible behavior is obtained for $\nu_u = 0.5$. However, taking $\nu_u = 0.5$ leads to singularity of the stiffness matrix (Equation 6.8). In order to avoid numerical problems caused by an extremely low compressibility, by default, the PLAXIS program considers ν_u as 0.495, which makes the undrained soil body slightly compressible. Consequently, for undrained material behavior a bulk modulus of water is automatically added to the stiffness matrix. Its value is determined by Equation (6.8).

$$\frac{K_w}{n} = \frac{3(\nu_u - \nu')}{(1-2\nu_u)(1+\nu')} K' = 300 \frac{0.495 - \nu'}{1+\nu'} K' \tag{6.8}$$

where n is porosity

To ensure realistic computational results, the bulk modulus of the water must be high enough when compared with the bulk modulus of the soil skeleton, i.e. $K_w >> n K'$. This condition is sufficiently ensured by requiring $\nu' \leq 0.35$.

The simulation of undrained material behavior on the basis of effective parameters is very convenient when such parameters are available. This enables undrained calculations to be executed with explicit distinction between effective stresses and (excess) pore pressures. For soft soil projects such as those in Bangkok, accurate data on effective parameters are not always be available. Instead, in situ tests and laboratory tests are usually performed to obtain undrained soil parameters. In these situations measured undrained Young's modulus can be easily converted into effective Young's modulus by:

$$E' = \frac{2(1+\nu')}{3} E_u \tag{6.9}$$

Undrained shear strengths, however, cannot easily be used to determine the effective strength parameters φ and c. In this case, PLAXIS offers the possibility of an

undrained analysis with direct input of the undrained shear strength as described in the next section.

6.11.3 Undrained Analysis with Undrained Parameters

With this alternative, the non-porous option is selected to simulate the undrained behavior. This means that the grain solid of soil and pore water are considered as a unique body, and they directly enter undrained elastic properties $E = E_u$ and $\nu = \nu_u = 0.495$ in combination with the undrained strength properties $c = c_u$ or S_u and $\varphi = \varphi_u = 0°$. In this case a total stress analysis is performed without distinction between effective stresses and pore pressures. Therefore, the output of effective stresses are interpreted as total stresses and all the pore water pressures of the non-porous layers are equal to zero.

As the available soil data are limited, this option is the most appropriate to be used for simulation of the tunnel excavation as well as for a study on the behaviors of ground and structural movements in response to tunneling for this research.

6.11.4 Relationship between Undrained Shear Strength and Soil Stiffness

It has been known up till now that the subsoil stiffness is not a constant value, but it depends on strain levels. Mair (1993) reported the changes of soil stiffness with different working shear strain levels for various structural systems (Figure 6.6). The typical working range of tunnels is between 0.1% and 1%.

Shibuya et al. (2001) established the relationship between shear strain and the ratio of in-situ secant shear modulus ($G_{sec(in\text{-}situ)}$) to undrained shear strength obtained from monotonic triaxial ($S_{u(MTX)}$) and field vane shear tests ($S_{u(FVS)}$) for Bangkok clay as shown in Figure 6.7. The average values of $G_{sec(in\text{-}situ)}/S_{u(MTX)}$ in soft clay corresponding to 0.1% and 1% of shear strain were about 230 and 70 respectively while $G_{sec(in\text{-}situ)}/S_{u(FVS)}$ were about 315 and 80. However, these average values in stiff clay found were about 530 and 100 for both $G_{sec(in\text{-}situ)}/S_{u(MTX)}$ and $G_{sec(in\text{-}situ)}/S_{u(FVS)}$.

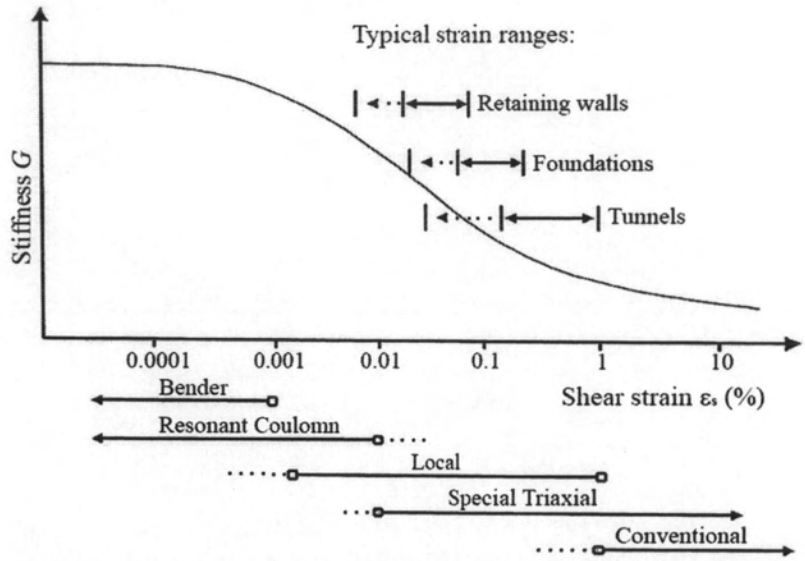

Figure 6.6 Typical shear modulus and shear strains for different geotechnical works (Mair, 1993)

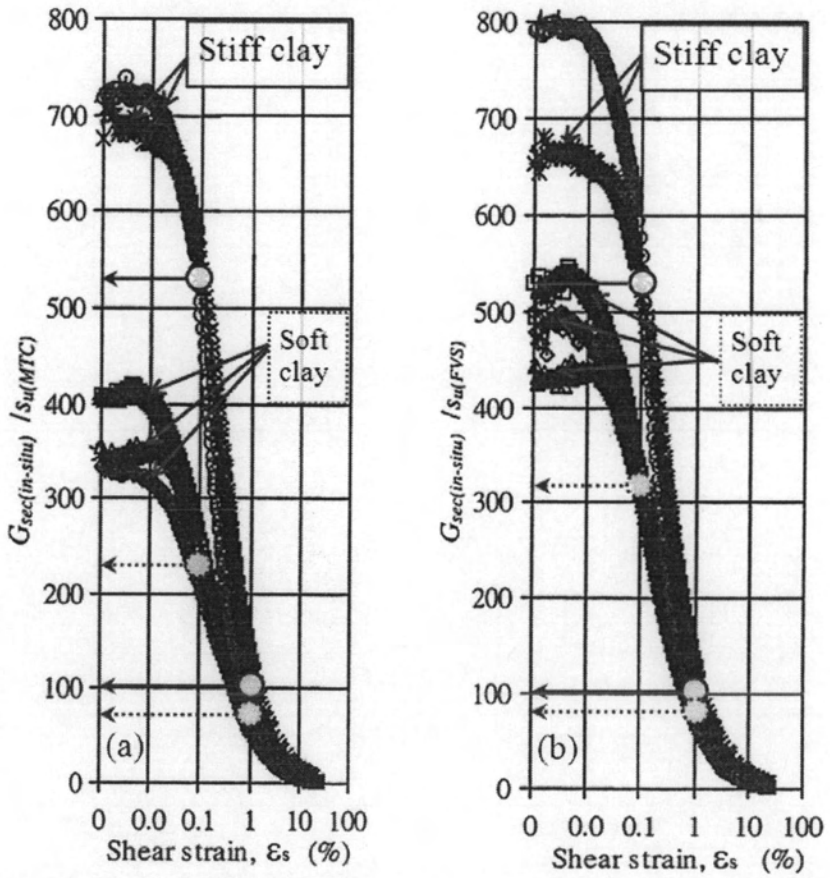

Figure 6.7 Variations of $G_{sec(in\text{-}situ)}/S_u$ with shear strains; (a) S_u from MTX, (b) S_u from field vane shear tests (Shibuya et al., 2001)

It is noticeable that the determination of $G_{sec(in\text{-}situ)}$ was based on the results of monotonic undrained triaxial compression and the in-situ seismic cone penetration tests (Shibuya and Tamrakar, 1999 and 2003; Shibuya et al., 2001). For the undrained shear condition of clay sample, the secant shear modulus (G_{sec}) is linked to the secant Young's modulus (E_{sec}) by the relation $G_{sec} = E_{sec}/3$. Consequently, the average values of E_u/S_u in soft clay corresponding to 0.1% and 1% shear strain were about 690 and 210 respectively for triaxial test; however, these values slightly increased to 945 and 240 for field vane shear tests. Moreover, these ratios (E_u/S_u) became 1590 and 300 for stiff clay layer.

Similarly, Teparaksa (2005a and b) also presented the correlation between soil stiffness in terms of shear modulus to undrained shear strength (G/S_u) and shear strain for soft and stiff Bangkok clays as shown in Figure 6.8. The curves were taken as the average of all the results given by six numbers of self boring pressuremeter tests for soft and stiff clay layers, which were performed during the design of the first MRTA blue line in Bangkok city and reported by Teparaksa and Heidengren, (1999). The values of G/S_u in soft clay corresponding to 0.1% and 1% of shear strain were about 132 and 55 respectively while the ratios of G/S_u in stiff clay were increased to about 211 and 78.

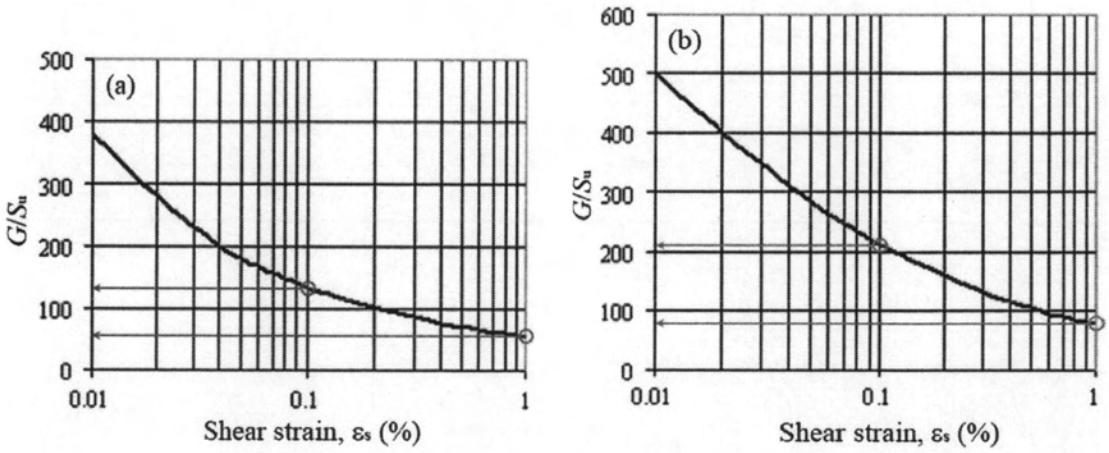

Figure 6.8 Shear modulus of Bangkok clays (a) soft clay and (b) stiff clay (Teparaksa, 2005a and b)

As the self boring pressuremeter tests were performed in undrained condition for each clay layer, the same relation between shear modulus (G) and the undrained Young's modulus (E_u) is still applicable, $G = E_u/3$. Accordingly, the values of E_u/S_u in

soft clay for shear strain of 0.1% and 1% were about 396 and 165 respectively and these ratios became 633 and 234 for stiff clay layer.

Although the ratios of E_u/S_u, which are in the ranges of shear strain between 0.1% to 1% , obtained from Figure 6.8 are smaller than those of Figure 6.7 for both soft and stiff clays, the values of these ratios are always greater for stiff clay than for soft clay.

Within the range of shear strain 0.1% and 1%, Teparaksa and Heidengren, (1999) and Teparaksa, (1999) carried out the back analysis, which was based on 2D-FEM program with Mohr-Coulomb soil model, and found that the appropriate Young's modulus ratios (E_u/S_u) for estimating the ground displacement due to EPB shield tunneling in Bangkok were 240 and 480 for soft and stiff clays, respectively. These ratios are located in the same intervals as what yielded from laboratory (monotonic undrained triaxial compression) and in-situ (seismic cone penetration) as well as from self boring pressuremeter tests described previously. In addition, Teparaksa (2005a) used the values of drained modulus E' (kN/m^2) = 2000.N_{60}, where N_{60} was the SPT N-value at 60% energy ratio, for silty sand to design a tunnel boring in Bangkok subsoils. Therefore, for the soil stiffness, E_u/S_u and E', 240 and 480 for soft and stiff clays respectively, and 2000.N_{60}, are used in this study.

Table 6.1 presents the structural properties at Klongtan Bridge and BTS-Sukhumvit areas, which are used in the 2D FEM simulation. In addition, Tables 6.2 and 6.3 show the soil parameters for FEM analyses at the two studied areas.

Table 6.1 Structural properties for FEM analyses at Klongtan Bridge and BTS-Sukhumvit areas

Material	γ_c (kN/m^3)	d_{eq} (m)	E_c (kN/m^2)	ν_c (-)
Tunnel lining	23.544	0.275	29842020.00	0.16
Pile caps of shophouses	23.544	0.400	23592188.30	0.16
Concrete piles of shophouses	23.544	0.200	23592188.30	0.16
Pile caps of Klongtan bridge	23.544	1.000	23592188.30	0.16
Concrete piles of Klongtan bridge	23.544	0.350	23592188.30	0.16
Pile caps of BTS sky train	23.544	1.800	29842020.00	0.16
Concrete piles of BTS sky train	23.544	0.866	29842020.00	0.16

Table 6.2 Soil parameters for FEM analyses at Klongtan Bridge area

Depth (m)	Soil layer	γ (kN/m^3)	$S_{u(FVS)}$, S_u (kN/m^2)	φ (^{o})	E_u, E' (kN/m^2)	ν(-)	K_o, K
0.00- 2.00	Weathered crust	17.5	30.0	-	10800	0.350	0.650
2.00- 14.00	Soft clay, CH	15.7	24.0	-	5760	0.495	0.837
14.00- 20.50	Stiff silty clay, CL	19.0	80.6	-	38688	0.495	0.620
20.50- 22.00	Medium dense silty sand, SC	20.0	-	30	33354	0.350	0.500
22.00- 24.00	Very stiff silty clay, CL	20.0	135	-	64800	0.495	0.561
24.00- 37.50	Dense silty sand, SM-SP	20.0	-	35	70632	0.350	0.426
37.50- 40.00	Hard silty clay, CL	20.5	221.0	-	106080	0.495	0.656

Table 6.3 Soil parameters for FEM analyses at BTS-Sukhumvit area

Depth (m)	Soil layer	γ_t (kN/m^3)	$S_{u(FVS)}$, S_u (kN/m^2)	φ (°)	Eu, E' (kN/m^2)	ν(-)	K_o, K
0.00- 3.00	Weathered crust	17.5	30.0	-	10800	0.35	0.67
3.00- 12.00	Soft clay, CH	15.7	20.5	-	4920	0.495	0.854
12.00- 15.00	Medium stiff clay, CH	17.0	46.6	-	16776	0.495	0.7
15.00- 22.50	Stiff silty clay, CL	19.0	97.2	-	46656	0.495	0.6
22.50- 25.50	Very stiff silty clay, CL	20.3	186.0	-	89280	0.495	0.572
25.50- 30.00	Hard silty clay, CL	20.5	265.5	-	127440	0.495	0.544
30.00- 34.50	Very stiff silty clay, CL	20.0	141.0	-	67680	0.495	0.63
34.50- 37.50	Dense silty sand, SM-SP	20.0	-	35	70632	0.35	0.426
37.5- 48.00	Stiff silty clay, CL	17.5	94.0	-	45120	0.495	0.66
> 48.0	Very dense sand, SM-SP	20.0	-	40	98100	0.35	0.357

In both tables, Tables 6.2 and 6.3, the coefficients of lateral earth pressure K and K_o are determined based on the procedure mentioned in section 6.11.5.

6.11.5 Determination of Coefficient of Lateral Earth Pressure

The coefficient of lateral earth pressure has been known as the effective and total coefficient. In an undisturbed ground, the ratio of the horizontal to vertical effective stress is defined as the coefficient of lateral earth pressure at rest, K_o:

$$K_o = \frac{\sigma'_h}{\sigma'_v} \tag{6.10}$$

The value of K_o can vary between about 0.2 and 6 (Coduto, 2001). Typical values are 0.35 and 0.7 for normally consolidated soils and between 0.5 and 3 for overconsolidated soils. The most accurate way to determine K_o is by measuring σ_h in-situ using methods such as the pressuremeter, dilatometer, or stepped blade, and combining it with computed value of σ_v and pore water pressure, u.

In practice, the value of K_o for a normally consolidated soil is often assumed to be related to the effective friction angle φ' by the empirical expression of Jaky (1944):

$$K_{oNC} = 1 - \sin\varphi' \tag{6.11}$$

The most common method of assessing K_o at any degree of consolidation is given by Equation 6.12 (Mayne and Kulhawy, 1982). This formula is applicable only when the ground surface is level:

$$K_o = (1 - \sin\varphi').OCR^{\sin\varphi'} \tag{6.12}$$

in which OCR is the overconsolidation ratio and other parameters have been mentioned previously.

Shibuya and Tamrakar (1999) mentioned that the values of $K_{o(NC)}$ for Bangkok soft clay ranged from 0.70 to 0.75; however, the value of $K_{o(NC)}$ for stiff clay were lower than those of soft clay; i.e., over a range from 0.52 to 0.6. In both clays, the K_o was linked to OCR by the expression

$$K_o = K_{oNC}.(OCR)^{0.5} \tag{6.13}$$

Interestingly, the values of K_o for a cohesionless soil are bounded by:

$$\frac{1-\sin\varphi'}{1+\sin\varphi'} < K_o < \frac{1+\sin\varphi'}{1-\sin\varphi'} \qquad (6.14)$$

In the case where the undrained analysis is performed, the total coefficient of lateral earth pressure K will be needed and it can be determined by the Equation 6.15.

$$K = \frac{\sigma_h}{\sigma_v} = \frac{K_o + \frac{u}{\sigma_v'}}{1 + \frac{u}{\sigma_v'}} \qquad (6.15)$$

where u, σ_h, σ'_h, σ_v and σ'_v are pore water pressure, total and effective horizontal and vertical stresses respectively.

For a soil deposit with the water table at the surface and bulk density ρ, the coefficient K could be determined from Equation 6.16 (Pender, 1980).

$$K = K_o - \frac{\rho_w}{\rho}.(K_o - 1) \qquad (6.16)$$

in which ρ_w is the water density.

6.12 PLAXIS Used in Previous Research Studies

PLAXIS, an FEM program, was initially developed to analyze the problems associated with river embankments on soft soils in Holland. This 2D finite element code started to be developed in 1987 at the Technical University of Deft as an initiative of the Dutch Department of Public Works and Water Management. After 10-year development, the Windows version was available in 1998 (Brinkgreve, 2002). Until now, many features related to geotechnical problems have been incorporated into the program that makes it broadly used in the geotechnical works. Moreover, among the six soil models available in the program, the Mohr Coulomb seems the most attractive model to use for both designers and researchers.

Some of the examples where Mohr Coulomb and PLAXIS are used as one package to analyze the geotechnical problems, specifically to study the behaviors of

ground movement responding to tunneling works are briefly given in the following paragraphs.

Teparaksa and Heidengren (1999) and Teparaksa (1999) performed a back analysis by using 2D PLAXIS with the elastic perfectly-plastic failure criteria of Mohr Coulomb model to study the interaction between soil and structures during the EPB shield tunneling and subway station box excavation in Bangkok. The aspects for the design of these structures are also mentioned. The same soil model and finite element code were also used to design the extension portion of Bangkok blue line subway (Teparaksa et al., 2006).

Vermeer et al. (2002) carried out an analysis on a circular NATM tunneling based on the program of PLAXIS 3D tunnel, and the ground surface settlement trough was well compared with empirical Gaussian curve and 2D analysis result. The Mohr Coulomb model was considered in the programs, both 2D and 3D PLAXIS. Their finding intends to suggest a fast method for 3D tunnel analysis, i.e. NATM tunnels.

Bonnier et al. (2002) used 2D and 3D PLAXIS to predict the loads on circular tunnel lining constructed by NATM method. The constitutive soil model was indicated by Mohr Coulomb soil parameters. In order to do the comparison between the internal forces obtained from both 2D and 3D analyses, the simulation of tunnel construction method based on β-value was also applied to 2D model. Although the normal forces given by 2D analysis are lower than the average value of the ones from 3D, the 2D value is still realistic and reliable. Moreover, the 2D bending moments appear to match the average ones from a 3D analysis quite well. As the time required for 2D simulation is relatively short; therefore, this approach is still retained within geotechnical research as well as in engineering practice.

Koungelis and Augarde (2004) studied three possibilities of two tunnel constructions, parallel and piggy-back geometries, based on 2D PLAXIS. Then some guidance on the possible effects between these tunnels were provided in the case where a particular soil profile was given with the basic parameters of Mohr Coulomb model.

6.13 Analysis Method of this Study

A systematic research procedure yielding a fruitful result mainly depends on a research design and the method of analysis which have been well planned in prior.

This section, therefore, depicts the necessity of the field monitored data used in this research and the procedures that the analyses are carried out. This leads to the final results in the next chapter.

6.13.1 Selection of Field Monitored Data

All analyses in this research are mainly related to the final short-term condition, which is known as the end of excessive pore water pressure dissipation. In this regard, Srisirirojanakorn (2004) pointed out an interval when the shield passed test sections for the 2000 Evanston tunnel (ET2) as between 10 and 13 days or 91 (298 ft) and 47.5 m. (156 ft.), respectively. Similarly, Phenwej et al. (2006) plotted the changing of subsurface settlement with time in which the significant settlements happened until about 20 days after the shield passed the control section. However, they revealed that in some cases, settlements in soft clay layers, almost 100 percent of short term settlements reached after three to four months.

Accordingly, the three-month data was selected. However, there was no significant difference between one-week, two-week and three-month data (Appendix B). In addition, the field monitored data used in this research was limited to the ground surface settlement arrays, subsurface settlements from borehole extensometers, building settlement points and lateral displacements from inclinometer.

6.13.2 Classification of Ground and Structural Movements

The behaviors of ground surface and subsurface movements as well as structural settlements along the direction of tunnel excavation were classified according to each position of the TBM in respect to the monitored section. These behaviors are extensively described in sections 7.1.1 and 7.2 in the next chapter, Chapter VII.

6.13.3 Empirical Method of Analysis

The monitored data of ground surface settlement arrays were plotted against the lateral distance from the tunnel centerline, and then the volume of ground surface settlement trough per unit length (V_s) was estimated. Therefore, the volume of ground

loss (V_L) expressed in percentage and the trough width parameter (i) could be determined by using Equation (4.6). Subsequently, the ground surface settlement trough could be satisfactorily reproduced based on Equation (4.1).

Moreover, the obtained volume of ground loss (V_L) was later on served as the input of the tunnel contraction for FE analysis.

6.13.4 FE Analysis

6.13.4.1 Model Configuration

For this study, it was the tunnel excavation and a 3D problem so the analysis model for this research was set to plane strain condition. In order to increase the accuracy in deformation analysis, the 15-node triangular soil element consisting of 15 nodes and 12 stress points were also considered in the analysis model. Moreover, the very fine mesh was generated for the whole model geometry and three times of mesh refinement were applied to the clusters inside the tunnel.

Since the available soil data were limited, the constitutive soil model based on elasto-plastic failure criteria of Mohr-Coulomb was the most appropriate to use in this research. In addition, the non-porous option was set to all the cohesive soil while sand and silty sand was considered as drained materials (Tables 6.2 and 6.3). With these settings, there was no ground water flowing in the clay layers and any consolidation could happen in the whole analysis. On the other hand, the tunnel lining and structural elements were simulated as line elements based on elastic properties (Table 6.1).

As the site conditions of the flood diversion tunnel are not symmetric, the full tunnel cross sections were considered in the analyses. In addition in the case where the simulation must be done for the sections, which are not far from one to another and with similar field conditions such as those along the Klongtan bridge, the analysis configurations of each bridge footing and the existing old shophouses based on 2D FEM are the same whereas only the positions of the structures to the tunnel center line are adjusted according to the real analysis sections.

6.13.4.1 Simulation of Tunnel Excavation

The different steps of calculation were performed, based on 2D-FEM program, to simulate the 3D advancement of the tunnel. The 2D-FEM simulation of tunnel construction by means of EPB shield machine could be performed in four phases:

1.) *Initial condition determination:* The initial conditions are described with initial in situ stress state and the initial configuration, and initial water pressures. The computation of initial conditions is done after the finite element mesh has been generated. The water pressures are easily generated based on the phreatic level while the initial stresses are calculated based on the K_o-procedure for the sand and silty sand layers and on the coefficient of total lateral earth pressure (K) for clay and silty clay layers.

2.) *The deformation and stresses induced by the existing structures and surcharges:* The deformation and stress state within the soil mass in this phase is calculated immediately after the initial conditions by activating all the existing structures and surcharges at the section under an analysis. Actually this phase is also a part of initial field conditions, which already exist on the site before the tunnel construction. Therefore the displacements happening during this phase are reset to zero for the next calculation phase. One can activate the existing structures and surcharges in two phases separately without any effect on the final deformation.

3.) *The tunnel excavation and installation of precast concrete segmental linings:* The tunnel excavation and installation of precast concrete segmental linings are simulated by deactivating the soil clusters inside the tunnel and activating the segmental linings, which have been created in the input of the model. In addition, the changes of water pressures inside the tunnel are also calculated.

4.) *The simulation of ground loss after passing of EPB:* The simulation of ground loss or contraction is done after the EPB shield machine passes. This ground loss is the result of several factors which are the over-cutting, different diameter of TBM and the permanent tunnel lining, and redistribution of stress in the soil mass surrounding the tunnel (Chapter IV for more detail).